Melatonin attenuates radiation-induced cortical bone-derived stem cells injury and enhances bone repair in postradiation femoral defect model

Wei Hu
PLAGH: Chinese PLA General Hospital
Jiawu Liang
PLAGH: Chinese PLA General Hospital
Song Liao
PLAGH: Chinese PLA General Hospital
Zhidong Zhao
PLAGH: Chinese PLA General Hospital
Yuxing Wang
PLAGH: Chinese PLA General Hospital
Xiaofei Mao
PLAGH: Chinese PLA General Hospital
Siwei Hao
PLAGH: Chinese PLA General Hospital
Yifan Wang
PLAGH: Chinese PLA General Hospital
Bin Guo (guobin1110@126.com)
PLAGH: Chinese PLA General Hospital https://orcid.org/0000-0002-2207-9405

Research

Keywords: Melatonin, Stem cells, Ionizing radiation, Bone regeneration

Posted Date: July 24th, 2021

DOI: https://doi.org/10.21203/rs.3.rs-737962/v1

Version of Record: A version of this preprint was published at Military Medical Research on December 1st, 2021. See the published version at https://doi.org/10.1186/s40779-021-00355-y.

Abstract

Background

Ionizing radiation poses a challenge to the healing of bone defects. Radiation therapy and accidental exposure to gamma-ray (γ-ray) radiation inhibit bone formation and increase the risk of fractures. Cortical bone-derived stem cells (CBSCs) are essential for osteogenic lineages, bone maintenance, and repair. This study aimed to investigate the effects of melatonin on postradiation CBSCs and bone defects.

Methods

CBSCs were extracted from C57/BL6 mice and were identified by flow cytometry. The effects of exogenous melatonin on the self-renewal and osteogenic capacity of postradiation CBSCs were detected *in vitro*. The underlying mechanisms in terms of genomic stability, apoptosis and oxidative stress-related signaling were further analyzed by western blotting, flow cytometry and immunofluorescence. Finally, the effects of melatonin on healing in postradiation bone defects were evaluated *in vivo* by micro-CT and immunohistochemical analysis.

Results

The radiation-induced reduced self-renewal and osteogenic capacity were partially reversed in postradiation CBSCs treated with melatonin. Melatonin maintained the genomic stability and apoptosis of postradiation CBSCs, and intracellular oxidative stress was decreased significantly while antioxidant-related enzymes were enhanced. Western blotting verified the anti-inflammatory effect of melatonin by downregulating the levels of IL-6 and TNF-α via extracellular regulated kinase (ERK)/nuclear factor erythroid 2-related factor 2 (NRF2)/heme oxygenase 1 (HO-1) signaling, distinct from its antioxidant effect via NRF2 signaling. *In vivo* experiments demonstrated that the newly formed bone in the melatonin plus Matrigel group had higher trabecular bone volume per tissue volume (BV/TV) and bone mineral density (BMD) values, and lower levels of IL-6 and TNF-α than those in the irradiation and the Matrigel groups.

Conclusions

This study suggested the potential of melatonin to protect CBSCs against γ-ray radiation and to assist the healing of postradiation bone defects.

Background

Gamma rays (γ-rays) are a type of ionizing radiation that have been applied widely in diagnostic radiography, radiation oncology, and military weapons [1]. Ionizing radiation has been found to be closely

associated with bone metabolism. Given its high calcium content, bone tissue is sensitive to ionizing radiation and absorbs nearly 40% more irradiation than the surrounding tissues [2]. The cumulative incidence rate of pelvic fracture in women has been reported to be up to 13% after radiotherapy, and for patients with lung cancer, post stereotactic body radiotherapy computing tomography imaging frequently reveals rib fractures [3, 4]. Therapeutic or accidental ionizing radiation exposure might induce disorders of bone remodeling including malignancy, avascular necrosis, arrest of bone growth, fracture, and osteopenia [5–7]. Although the harmful effects of ionizing radiation on bone have been widely accepted, the direct mechanisms of radiation-induced bone loss at the cellular level have not been well elucidated.

Cortical bone-derived stem cells (CBSCs) have been reported to possess increased clonal incidence, potency, and developmental capacity compared to their bone marrow-derived counterparts [8]. CBSCs with superior proliferative and differentiation capacities suggest their consideration as an alternate source for regenerative treatments [9]. Nonetheless, safe and effective treatment for postradiation bone damage is of considerable interest, and it is imperative to search for pharmacological approaches to treat postradiation bone damage. Collectively, therapeutic agents to treat irradiation are conventionally divided into five categories: sulfydryl compounds, cytokines, hormones, antioxidants, and traditional Chinese medicine [10–12].

In humans, the pineal gland mainly synthesizes and secretes the hormone N-acetyl-5-methoxytryptamine (Melatonin). Melatonin acts as an autocrine, paracrine, and endocrine hormone to regulate the circadian rhythms of neighboring and distant cells [13]. Melatonin also acts as a potent free radical scavenger to remove singlet oxygen, superoxide anion radicals, and hydroperoxide efficiently. It induces antioxidative enzymes, such as superoxide dismutase, glutathione peroxidase, and catalase through a cascade reaction [14]. Zetner et al. have conducted a systematic review and found that exogenous melatonin can reduce oxidative stress and inflammation in all studied animal tissues with improvement in the 30-day survival [15]. Additionally, melatonin modulates immune responses and exhibits anti-aging properties. Serin et al. have shown that administration of 100 mg/kg of melatonin prior to γ-rays exposure to the lungs of rats reduced alveolar edema, macrophage and lymphocyte infiltration [16]. Notably, melatonin is considered to stimulate osteogenic and chondrogenic differetiation but inhibit adipogenic differentiation in BMMSCs [17]. Dong et al. have demonstrated that melatonin can drive the commitment and differentiation of mesenchymal stem cells into osteogenic lineages via Neuropeptide Y signaling [18]. However, little is known about the therapeutic effect of melatonin in postradiation bone.

In this study, we hypothesized that melatonin would alleviate radiation-induced oxidative stress and maintain the osteogenic capacity of postradiation CBSCs. We further examined whether melatonin was helpful to repair postradiation bone defects and investigated the intrinsic molecular mechanisms.

Methods

Animals

Male C57/BL6 mice aged 8 weeks were procured from Vital River Experimental Animal Technology Co., Ltd. (Beijing, China). All animal experiments were approved by the Animal Ethics Committee of the Academy of Military Medical Sciences (Ethical Approval Number: IACUC-DWZX-2020-719). All surgical and irradiation procedures were performed under anesthesia, and animal suffering was minimized as much as possible.

Irradiation

A Cobalt-60 radiation facility at the Institute of Radiation Medicine, the Academy of Military Medical Sciences (Beijing, China), was used for irradiation. 6 Gy γ-rays at dose rates of 0.5–1 Gy/min were applied to cells or mice. Except the hind legs and lower abdomens, the whole mouse body was obstructed and protected from γ-rays using lead blocks.

Isolation, culture and identification of CBSCs

CBSCs were isolated as previously described [19]. Briefly, the femurs were extracted after mice execution. Sterile scissors were used to remove the epiphyses just below the end of the marrow cavity, followed by thorough washing of the bone cavities using alpha minimal essential medium (α-MEM) until the bones appeared pale. The compact bones were excised into chips of approximately 3 mm^3, and were transferred into Eppendorf tubes containing 1 ml of α-MEM and 1 mg/ml of collagenase II at 37 °C for 1 h, followed by incubation at 37 °C in a 5% CO_2 incubator. Peridinin chlorophyll protein complex (PerCP)-conjugated anti-mouse CD45 antibodies and Phycoerythrin (PE)-conjugated anti-mouse spinocerebellar ataxia type 1 protein (Sca-1), CD140a, CD105, CD80, CD44, CD31, and CD11b antibodies (eBioscience, Cambridge, UK) were used to stain CBSCs for 30 min in the dark according to the manufacturer's instructions. Then flow cytometry analysis was performed using a FACSCalibur flow cytometer (BD Biosciences, San Jose, CA, USA) and data were analyzed using the FlowJo V10 software (BD Biosciences). For melatonin treatment, various concentrations of melatonin treated CBSCs from 1 hour after irradiation for 24 h.

Analysis of colony-forming unit fibroblast (CFU-F)

CBSCs were seeded into 6-well plates at a density of 200 cells/well and cultured for 12 days. When visible colonies were formed, the colonies were fixed with 20% methanol, stained with 0.1% crystal violet, and photographed. Finally, positive colony formation (more than 50 cells/colony) was determined by counting under a microscope.

Osteogenesis and adipogenesis assay

The complete media for differentiation were purchased from Cyagen Biosciences (Santa Clara, CA, USA). Total RNA was extracted for quantitative real-time reverse transcription polymerase chain reaction (qRT-PCR) after osteogenic and adipogenic differentiation. Alkaline phosphatase staining was performed according to the manufacture's instructions (Beyotime) after two weeks of osteogenic differentiation. Alizarin red S staining was performed to assess calcium deposition after three weeks of osteogenic

differentiation. CBSCs were fixed and lipid droplets were visualized using filtered Oil red O after two weeks of adipogenic differentiation.

Cell apoptosis analysis

An Annexin V-Allophycocyanin (APC)/7-Aminoactinomycin D (7-AAD) apoptosis detection kit (Keygen, Jiangsu, China) was used to determine apoptosis of CBSCs. Briefly, 2×10^5 cells in suspension were centrifuged at 1000×g for 5 min and the supernatant was discarded. Thereafter, the cells were re-suspended in 500 μl of binding buffer. Then, 5 μl of APC and 5 μl of 7-AAD were added to the suspension and incubated for 15 min at room temperature in the dark. Cell apoptosis was determined by flow cytometry for 2×10^4 events at a flow rate not exceeding 500 cells per second and the data were analyzed using the FlowJo V10 software.

Determination of ROS, MDA, SOD Levels and GSH/GSSG ratio

Intracellular reactive oxygen species (ROS) levels were investigated using a ROS Assay Kit (Beyotime). Briefly, CBSCs were seeded at 10^5 cells in 25 mm^3 culture flasks. Then the medium was replaced with serum-free medium containing a Dichlorofluorescein-diacetate (DCFH-DA) probe at a final concentration of 10 μmol/L and placed in the dark for 30 min. The cells were then harvested and fluorescence detection was performed using flow cytometry at an emission wavelength of 525 nm and an excitation wavelength of 488 nm. The measurement of intracellular malondialdehyde (MDA), superoxide dismutase (SOD) levels and glutathione/oxidized glutathione (GSH/GSSG) ratio was performed according to the manufacture's instructions using a MDA assay kit (Ray Biotech), a SOD assay kit (Beyotime) and a GSH/GSSG assay kit (Beyotime).

qRT-PCR

The TRIzol reagent (Invitrogen, Carlsbad, CA, USA) was used to isolate total RNA from the cells. A reverse transcription kit (Yishan, Shanghai, China) was then used to reverse transcribe the RNA to cDNA. The quantitative real-time PCR (qPCR) reaction was performed according to the reagent instructions of the UltraSYBR Mixture (CWBIO, Beijing, China), using the cDNA as the template and the following reaction program: 95 °C for 2 min, followed by 40 cycles of 95 °C for 15 sec, 60 °C for 30 sec and 72 °C for 30 sec. Sangon Biotech (Shanghai, China) synthesized all the primers. The primers used in this study are listed as follows (5'-3'): *Runx2*, sense, GACTGTGGTTACCGTCATGGC and anti-sense, ACTTGGTTTTTCATAACAGCGGA; *Opn*, sense, ATCTCACCATTCGGATGAGTCT and antisense, TGTAGGGACGATTGGAGTGAAA; *Pparg*, sense, GGAAGACCACTCGCATTCCTT and antisense, GTAATCAGCAACCATTGGGTCA; *Cebpa*, sense, GCGGGAACGCAACAACATC and antisense, GTCA-CTGGTCAACTCCAGCAC. Relative gene expression was quantified using the $2^{-\Delta\Delta Ct}$ method [20].

Immunofluorescence

Cells were seeded at a density of 2×10^4/well into 12-well plates plated with cell-climbing slices. Paraformaldehyde was then used to fix the cells and 0.5% Triton X-100 was used to permeabilize them. Goat serum was then used to block non-specific binding to the cells before incubation with antibodies against gamma H2A histone family, member X (γH2AX; 1:200; CST, Danvers, MA, USA) overnight at 4 °C. The cells were then incubated with secondary antibodies conjugated to a fluorescent dye. Nuclear counterstaining was achieved using 4',6-diamidino-2-phenylindole (DAPI) at room temperature for 15 min. The coverslips with the cells were inverted on glass slides and fluorescence was assessed under a laser confocal microscope.

Western blotting analysis

Radioimmunoprecipitation assay (RIPA) lysis buffer (Beyotime, Shanghai, China) with 1 mM phenylmethanesulfonylfluoride (PMSF) was used to lyse the cells. Nuclear and Cytoplasmic Extraction Reagents (Thermo Scientific, Wilmington, DE, USA) were used to extract the nucleoproteins. SDS-PAGE (7.5–10% polyacrylamide gels) was used to separate the proteins, which were then transferred to polyvinylidene fluoride (PVDF) membranes (Thermo Scientific). Next, the membranes were blocked with 5% skim milk for 1 h and then incubated with the primary antibodies (1:1000) (CST) at 4°C overnight, followed by incubation with secondary antibodies (1:2000) (CST) at room temperature for 2 h. The immunoreactive protein bands were visualized using an enhanced chemiluminescence (ECL) kit (Thermo Scientific). A Luminescent Image Analyzer LAS4000 (Fuji Film, Tokyo, Japan) and ImageJ software (NIH, Bethesda, MD, USA) were used to detect and quantify the protein band signals. U0126 ERK pathway inhibitor was from Sigma-Aldrich (Danvers, MA, USA). ML385 NRF2 pathway inhibitor was purchased from MedChemExpress (Shanghai, China).

Femoral bone defect models

At 1 hour after irradiation, the mice were subjected to bone defect surgery. A femoral defect (1.5 mm diameter and 1 mm depth) was generated at the distal third of the femur as previously described [21]. Surgically treated, nonirradiated mice were used as blank controls. Melatonin was first diluted in absolute ethanol and then mixed and diluted with Matrigel at 4 °C to achieve a concentration of 100 μM. Matrigel presents as liquid form at 4 °C and in a semi-solid form at 37 °C. A 10 μL aliquot of Matrigel mixed with melatonin was injected into the postradiation femoral defect. The same volume of Matrigel without melatonin was used as a control. At 4 weeks after surgery, the mice were sacrificed, and micro-CT analysis and pathological evaluation of the harvested femurs were performed.

Micro-CT scan

The femur samples were fixed in formaldehyde for 24 h, and then placed in a 50 mm diameter tube that was oriented perpendicular to the scanning axis. Bone samples were then scanned using a Quantum GX micro-CT imaging system (PerkinElmer, Waltham, MA, USA) using the following settings: 70 kV, 100 μA and 14 min exposure time. A selected area (27 mm^3) of the three-dimensional reconstruction was centered at bone drilling site, followed by determination of the bone mineral density (BMD) and trabecular bone volume per tissue volume (BV/TV).

Hematoxylin-eosin staining, Masson staining and immunohistochemistry

Femurs were obtained, fixed in formaldehyde for 24 h, decalcified for 3 weeks, and embedded in paraffin. Femur sections were deparaffinized in xylene, dehydrated in ethanol and rinsed with tap water. Then stained those sections with haematoxilin and eosin solution each for 5 min (HE staining) or Lichun red magenta, phosphomolybdic acid, aniline blue solution each for 5 min (Masson staining). The sections for immunohistochemistry (IHC) analysis were subjected to the same dehydration protocol before antigen retrieval. TNF-α and IL-6 primary antibodies (1:100) were added to the sections, which were incubated overnight at 4 °C. The next day, the sections were incubated with secondary antibody labeled with horseradish peroxidase at 37 °C for 50 min. Diaminobenzidine was added to sections for approximately 10 min for color development. The sections were then counterstained with hematoxylin, dehydrated, incubated with xylene to make them transparent. All sections were sealed with neutral balsam followed by observation under an optical microscope.

Statistical analysis

The mean ± the standard deviation (SD) from at least three independent experiments was used to represent all the quantitative variables in the present study. GraphPad Prism 6.02 (GraphPad software Inc., San Diego, CA, USA) was used to carry out the statistical analyses. One-way analysis of variance (ANOVA) was used to compare the data from multiple groups. Statistical significance was accepted at a P value less than 0.05.

Results

Melatonin alleviated radiation-induced the loss of self-renewal and osteogenic capacity of CBSCs

We extracted and cultured cortical bone-derived stem cells (CBSCs) from femurs according to previous protocols (Fig. 1a). The results for CBSCs characterization showed that CBSCs were positive for markers CD44, CD80, CD105, CD140a and Sca-1, but negative for markers CD11b, CD31 and CD45 (Fig. 1b). To test if melatonin could affect radiation-induced injury, CBSCs received a single dose of 6 Gy γ-ray radiation with various concentrations of melatonin treatment. The radiation-induced destructive effect on self-renewal ability of CBSCs was demonstrated, and 100 μM melatonin increased colony formation significantly compared to IR group (Fig. 1c,1d). Furthermore, the expression of osteogenic gene markers after 100 μM melatonin treatment, including *Runx2* and *Opn*, were higher than those in the IR group. Conversely, radiation promoted adipogenic differentiation of CBSCs, and 100 μM melatonin significantly decreased the expression of adipogenesis-associated genes *Pparg* and *Cebpa* (Fig. 1e). In addition, alkaline phosphatase (ALP) staining and Alizarin red staining results agreed with the expression trend of osteogenic genes, but lipid droplets in IR group were fewer than those in the control and 100 μM melatonin treatment groups, which was likely related to changes of cell viability (Fig. 1f).

Melatonin maintained the genomic stability and apoptosis of postradiation CBSCs

γH2AX is a biomarker for DNA double strand breaks (DSBs), and Fig. 2a displayed fluorescence-labeled γH2AX in the nuclei of CBSCs. No significant difference was determined between IR and 1 μM melatonin treatment groups, but markedly decrease was observed in other melatonin treatment groups (Fig. 2b). Previous evidences showed that DSBs could induce apoptosis. Figure 2c.2d revealed that a similar trend was observed in apoptosis results by flow cytometry, and melatonin at 100 or 10 μM treatment significantly attenuated apoptosis of postradiation CBSCs. Correspondingly, the level of anti-apoptotic protein BCL-2 was increased by 100 or 10 μM treatment, which was opposite to the change trend of pro-apoptotic protein BAX (Fig. 2e).

Melatonin inhibited intracellular oxidative stress and enhanced antioxidant enzymes activity in postradiation CBSCs

We detected the amount of intracellular reactive oxygen species (ROS) through 2,7-dichloriflurescin (DCFH) staining. DCFH-DA was hydrolysed to produce DCFH in CBSCs, and oxidation of DCFH generated green fluorescence. As shown in Fig. 3a, postradiation CBSCs with or without 1 μM melatonin treatment presented brighter green fluorescence compared with the other groups. We further conducted quantitative analysis of ROS by flow cytometry. Irradiation triggered a surge in ROS levels, while 100 μM melatonin treatment remarkably decreased ROS production in postradiation CBSCs (Fig. 3b,3c). Figure 3d revealed that the melatonin-treated CBSCs after irradiation had a lower malondialdehyde (MDA) content, a higher level of superoxide dismutase (SOD) and a higher GSH/GSSG ratio in a concentration-dependent manner compared to IR group. Glutathione (GSH) exists in both reduced and oxidized states (GSSG), and GSH can be oxidized into GSSG by ROS. Since 100 μM melatonin treatment appeared good performance in postradiation CBSCs, the underlying mechanisms of protective effects were further investigated.

Melatonin exerted anti-inflammatory effect via the ERK/NRF2/HO-1 signaling and exerted antioxidant effect via NRF2 signaling

Melatonin promoted bone healing of postradiation femoral defect in vivo

To investigate the potential of melatonin for bone repair *in vivo*, a femoral bone defect model was established as previously described. Given its abundant extracellular matrix, BD Matrigel was chosen to be melatonin carrier which transformed from liquid-like to semi-solid-like state from 4 °C to 37 °C. Continuous new bone formation that bridged the cortical defects was observed in the control and the melatonin treatment groups. Quantitative results revealed that melatonin treatment achieved higher bone parameters, including bone volume per tissue volume (BV/TV) and bone mineral density (BMD) values,

than those in the IR and matriegel groups (Fig. 5a,5b). To substantiate the imaging results, representative histological and immunohistochemical sections of the healed bone defects were assessed. HE and Masson staining results showed a similar trend to micro-CT imaging findings indicating that melatonin was helpful to bone regeneration in the postradiation defect regions. Moreover, protein levels of pro-inflammatory cytokines TNF-α and IL-6 in the defect regions were significantly increased after irradiation, but were significantly decreased after melatonin treatment (Fig. 5c,5d).

Discussion

High radiation exposure from military nuclear weapons, nuclear accidents and radiotherapy elicits a series of complications, in which bone trauma and prolonged bone healing are rarely discussed before. The adverse effects of high-dose radiation on bone including sustained hypoxia of small blood vessels, decreased activity and abundance of osteocytes and osteoblasts, leading to bone hypoxia, cytopenia, angiopenia, and even radionecrosis [22, 23]. Here, we delivered a single sublethal dose of 6 Gy γ-ray radiation to CBSCs and bone defects, and of note, melatonin combined with Matrigel is utilized to maintain the self-renewal and osteogenic capacity of CBSCs *in situ* instead of allogeneic stem cells delivery.

From cell types points of view, stem or progenitor cells are more sensitive to ionizing radiation than non-proliferating and highly differentiated cells [24]. In the present study, it is difficult to tell which kind of stem cells, from cortical bone or bone marrow, play a more critical role in healing of femoral defects. In fact, the concept of skeletal stem cells were proposed and identified recently, and various markers were applied to differentiate subgroups of skeletal stem cells resided in growth plate, periosteum, etc [25–27]. Bone marrow-derive mesenchymal stem cells (BMMSCs) comprise a very heterogeneous cell mixture, only a fraction of which have stem properties. Previous studies have suggested that the cortical bone, rather than the bone marrow, might be a source of stem cells with more primitive characteristics [19, 28]. Moreover, due to enhanced proliferative, survival, and lineage commitment capacity, CBSCs have been used to cardiac wound healing [29].

Melatonin is well known for its potent antioxidant capacity, low toxicity, and wide distribution throughout the body [30, 31]. As a potent scavenger, melatonin and its metabolites can efficiently neutralize free radicals. Notably, melatonin is a amphiphilic peptide and has receptor-dependent and -independent functions [32]. The evolutionarily conserved hormone melatonin carries out its varied regulatory functions via binding to specific high affinity receptors, namely MT1/MT2, on the plasma membrane. It has been discovered that melatonin receptors MT1 and MT2 are expressed in BMMSCs [33]. Melatonin-mediated osteogenic promotion for BMMSCs has the potential to rely on MT2 receptor [34]. He et al. found that melatonin could better scavenger free radicals, enhance proliferation and osteogenic capacity, and downregulate the expression of matrix metalloproteinase in BMMSCs under the synergistic effect of extracellular matrix (ECM) [35]. Based on these evidences, we speculated that melatonin combined with Matrigel, which is rich in ECM and provides cells with space to form three-dimensional structures, might be beneficial for postradiation bone.

Many studies, till date, have investigated the molecular mechanisms underlying the immunoregulatory, antioxidative, and bone-supportive properties of melatonin. Pharmacological doses of melatonin inhibit INF-γ production in a range of 0.1 to 1 mM [36]. Oxidative stress and inflammation are interconnected pathophysiological processes associated with various inflammatory diseases [37]. We demonstrated that exogenous melatonin inhibited ROS production and attenuated the inflammatory response in postradiation bone. Khan et al. revealed that wogonin exerts an anti-inflammatory effect through the ROS/ERK/NRF2 signaling pathway [38]. NRF2 signaling acts as a master regulator of antioxidative stress, regulating antioxidant responsive gene expression and phase II detoxifying enzymes such as NQO1 and HO-1, which remove cytotoxic ROS to counteract oxidative damage in tissue [39]. Additionally, NRF2 deficiency enhanced inflammatory disorder susceptibility [40]. Likewise, our results suggested that the ERK/NRF2/HO-1 signaling pathway is activated by melatonin to suppress inflammatory responses. However, unlike NRF2 inhibitor, ERK inhibitor failed to block the rescue effect of melatonin in the present study. The other upstream regulatory molecules of NRF2, and the amphiphilic property of melatonin might provide explanation for this phenomenon.

Nonetheless, there are still several limitations that should be further addressed. Various doses of irradiation, the intervention time of melatonin after irradiation and associated outcomes should be further evaluated. Whether the receptor-dependent function of melatonin is related to inflammation and oxidative stress in postradiation CBSCs should be thoroughly investigated from a mechanistic aspect. The systemic application of melatonin might be a more reasonable approach to deal with total body irradiation and concomitant bone injury.

Conclusion

Melatonin as a therapeutic agent rescued the self-renewal and osteogenic capacity of postradiation CBSCs through maintaining genomic stability and apoptosis. Melatonin exerted anti-inflammatory effect through ERK/NRF2/HO-1 signaling pathway and exerted antioxidant effect via NRF2 signaling. Further analysis revealed that melatonin promoted the repair of postradiation bone defects and downregulated the levels of TNF-α and IL-6 in bone defect regions. Overall, our results suggested that melatonin might possess clinical benefits for the treatment of postradiation bone defects.

Abbreviations

CBSCs: Cortical bone-derived stem cells; MLT: Melatonin; IR: Irradiation; MDA: Malondialdehyde; CFU-F: Colony-forming unit fibroblast; ALP: Alkaline phosphatase; γH2AX: Gamma H2A histone family, member X; BCL-2: B-cell lymphoma-2; BAX: BCL2-associated X; SOD: Superoxide dismutase; GSH: Glutathione; ROS: Reactive oxygen species; HO-1: Heme oxygenase 1; ERK: Extracellular regulated kinase; NRF2: Nuclear factor erythroid 2-related factor 2; gel: Matrigel; BV/TV: Bone volume/tissue volume; BMD: Bone mineral density; BMMSCs: Bone marrow-derived mesenchymal stem cells; DSBs: DNA double-strand breaks; ECM: Extracellular matrix.

Declarations

Acknowledgments

The authors acknowledge Qian Wang, Sen Zhao, Yuning Zhang and Ying Zhou in Beijing Key Laboratory for Radiobiology for technical assistance.

Authors' contributions

WH and BG contributed to the idea and design of this research. WH, J-WL and SL collected the data. WH, SL, Z-DZ and Y-XW participated in the surgery of mice. S-WH and X-FM participated in the data analysis and interpretation. Y-FW contributed to the resourse of this research. WH, J-WL and BG participated in manuscript writing. BG provided the funds of this research. BG participated in the supervision of this research. All authors have read and agreed to the published version of the manuscript.

Funding

This research was funded by the National Natural Science Foundation of China (Grant number: 81470754) and the 13th Five-year Plan for Key Discipline Construction Project of PLA (Grant number: A350109).

Availability of data and materials

Not applicable.

Ethics approval and consent to participate

The study was conducted according to the guidelines of the Declaration of Helsinki, and approved by ethics committee of the Academy of Military Medical Science (ethical approval number: IACUC-DWZX-2020-719, valid from 18 July 2020 to 1 July 2021).

Consent for publication

Not applicable.

Competing interests

The authors declare that they have no competing interests.

References

1. Mehdipour A, Yousefi-Ahmadipour A, Kennedy D, Kazemi Arababadi M. Ionizing radiation and toll like receptors: A systematic review article. Hum Immunol. 2021;82:446–54.
2. Curi MM, Cardoso CL, de Lima HG, Kowalski LP, Martins MD. Histopathologic and Histomorphometric Analysis of Irradiation Injury in Bone and the Surrounding Soft Tissues of the Jaws. J Oral

Maxillofac Surg. 2016;74:190–9.
3. Schmeler KM, Jhingran A, Iyer RB, Sun CC, Eifel PJ, Soliman PT, et al. Pelvic fractures after radiotherapy for cervical cancer: implications for survivors. Cancer. 2010;116:625–30.
4. Nambu A, Onishi H, Aoki S, Tominaga L, Kuriyama K, Araya M, et al. Rib fracture after stereotactic radiotherapy for primary lung cancer: prevalence, degree of clinical symptoms, and risk factors. BMC Cancer. 2013;13:68.
5. Chandra A, Park SS, Pignolo RJ. Potential role of senescence in radiation-induced damage of the aged skeleton. Bone. 2019;120:423–31.
6. Pacheco R, Stock H. Effects of radiation on bone. Curr Osteoporos Rep. 2013;11:299–304.
7. Hui SK, Fairchild GR, Kidder LS, Sharma M, Bhattacharya M, Jackson S, et al. The influence of therapeutic radiation on the patterns of bone remodeling in ovary-intact and ovariectomized mice. Calcif Tissue Int. 2013;92:372–84.
8. Blashki D, Murphy MB, Ferrari M, Simmons PJ, Tasciotti E. Mesenchymal stem cells from cortical bone demonstrate increased clonal incidence, potency, and developmental capacity compared to their bone marrow-derived counterparts. J Tissue Eng. 2016;7:2041731416661196.
9. Kraus L, Ma L, Yang Y, Nguyen F, Hoy RC, Okuno T, et al. Cortical Bone Derived Stem Cells Modulate Cardiac Fibroblast Response via miR-18a in the Heart After Injury. Front Cell Dev Biol. 2020;8:494.
10. Singh VK, Newman VL, Romaine PL, Wise SY, Seed TM. Radiation countermeasure agents: an update (2011–2014). Expert Opin Ther Pat. 2014;24:1229–55.
11. Singh VK, Seed TM. The efficacy and safety of amifostine for the acute radiation syndrome. Expert Opin Drug Saf. 2019;18:1077–90.
12. Yahyapour R, Shabeeb D, Cheki M, Musa AE, Farhood B, Rezaeyan A, et al. Radiation Protection and Mitigation by Natural Antioxidants and Flavonoids: Implications to Radiotherapy and Radiation Disasters. Curr Mol Pharmacol. 2018;11:285–304.
13. Marqueze EC, Nogueira LFR, Vetter C, Skene DJ, Cipolla-Neto J, Moreno CRC. Exogenous melatonin decreases circadian misalignment and body weight among early types. J Pineal Res. 2021:e12750.
14. Segovia-Roldan M, Diez ER, Pueyo E. Melatonin to Rescue the Aged Heart: Antiarrhythmic and Antioxidant Benefits. Oxid Med Cell Longev. 2021;2021:8876792.
15. Zetner D, Andersen LP, Rosenberg J. Melatonin as Protection Against Radiation Injury: A Systematic Review. Drug Res (Stuttg). 2016;66:281–96.
16. Serin M, Gulbas H, Gurses I, Erkal HS, Yucel N. The histopathological evaluation of the effectiveness of melatonin as a protectant against acute lung injury induced by radiation therapy in a rat model. Int J Radiat Biol. 2007;83:187–93.
17. Wang B, Wen H, Smith W, Hao D, He B, Kong L. Regulation effects of melatonin on bone marrow mesenchymal stem cell differentiation. J Cell Physiol. 2019;234:1008–15.
18. Dong P, Gu X, Zhu G, Li M, Ma B, Zi Y. Melatonin Induces Osteoblastic Differentiation of Mesenchymal Stem Cells and Promotes Fracture Healing in a Rat Model of Femoral Fracture via

Neuropeptide Y/Neuropeptide Y Receptor Y1 Signaling. Pharmacology. 2018;102:272–80.

19. Zhu H, Guo ZK, Jiang XX, Li H, Wang XY, Yao HY, et al. A protocol for isolation and culture of mesenchymal stem cells from mouse compact bone. Nat Protoc. 2010;5:550–60.
20. Livak KJ, Schmittgen TD. Analysis of relative gene expression data using real-time quantitative PCR and the 2(-Delta Delta C(T)) Method. Methods. 2001;25:402–8.
21. Liang JW, Li PL, Wang Q, Liao S, Hu W, Zhao ZD, et al. Ferulic acid promotes bone defect repair after radiation by maintaining the stemness of skeletal stem cells. Stem Cells Transl Med. 2021.
22. Costa S, Reagan MR. Therapeutic Irradiation: Consequences for Bone and Bone Marrow Adipose Tissue. Front Endocrinol (Lausanne). 2019;10:587.
23. Groenen KH, Pouw MH, Hannink G, Hosman AJ, van der Linden YM, Verdonschot N, et al. The effect of radiotherapy, and radiotherapy combined with bisphosphonates or RANK ligand inhibitors on bone quality in bone metastases. A systematic review. Radiother Oncol. 2016;119:194–201.
24. Preciado S, Muntion S, Rico A, Perez-Romasanta LA, Ramos TL, Ortega R, et al. Mesenchymal Stromal Cell Irradiation Interferes with the Adipogenic/Osteogenic Differentiation Balance and Improves Their Hematopoietic-Supporting Ability. Biol Blood Marrow Transplant. 2018;24:443–51.
25. Cao Y, Buckels EJ, Matthews BG. Markers for Identification of Postnatal Skeletal Stem Cells In Vivo. Curr Osteoporos Rep. 2020;18:655–65.
26. Matsushita Y, Ono W, Ono N. Growth plate skeletal stem cells and their transition from cartilage to bone. Bone. 2020;136:115359.
27. Chan CKF, Gulati GS, Sinha R, Tompkins JV, Lopez M, Carter AC, et al. Identification of the Human Skeletal Stem Cell Cell. 2018;175:43–56 e21.
28. Smith SC, Zhang X, Zhang X, Gross P, Starosta T, Mohsin S, et al. GDF11 does not rescue aging-related pathological hypertrophy. Circ Res. 2015;117:926–32.
29. Mohsin S, Houser SR. Cortical Bone Derived Stem Cells for Cardiac Wound Healing. Korean Circ J. 2019;49:314–25.
30. Millet-Boureima C, Rozencwaig R, Polyak F, Gamberi C. Cyst Reduction by Melatonin in a Novel Drosophila Model of Polycystic Kidney Disease. Molecules. 2020;25.
31. Reiter RJ, Tan DX, Rosales-Corral S, Manchester LC. The universal nature, unequal distribution and antioxidant functions of melatonin and its derivatives. Mini Rev Med Chem. 2013;13:373–84.
32. Chen D, Zhang T, Lee TH. Cellular Mechanisms of Melatonin: Insight from Neurodegenerative Diseases. Biomolecules. 2020;10.
33. Slominski RM, Reiter RJ, Schlabritz-Loutsevitch N, Ostrom RS, Slominski AT. Melatonin membrane receptors in peripheral tissues: distribution and functions. Mol Cell Endocrinol. 2012;351:152–66.
34. Pytka K, Mlyniec K, Podkowa K, Podkowa A, Jakubczyk M, Zmudzka E, et al. The role of melatonin, neurokinin, neurotrophic tyrosine kinase and glucocorticoid receptors in antidepressant-like effect. Pharmacol Rep. 2017;69:546–54.

35. He F, Liu X, Xiong K, Chen S, Zhou L, Cui W, et al. Extracellular matrix modulates the biological effects of melatonin in mesenchymal stem cells. J Endocrinol. 2014;223:167–80.
36. Radogna F, Diederich M, Ghibelli L. Melatonin: a pleiotropic molecule regulating inflammation. Biochem Pharmacol. 2010;80:1844–52.
37. Khansari N, Shakiba Y, Mahmoudi M. Chronic inflammation and oxidative stress as a major cause of age-related diseases and cancer. Recent Pat Inflamm Allergy Drug Discov. 2009;3:73–80.
38. Khan NM, Haseeb A, Ansari MY, Devarapalli P, Haynie S, Haqqi TM. Wogonin, a plant derived small molecule, exerts potent anti-inflammatory and chondroprotective effects through the activation of ROS/ERK/Nrf2 signaling pathways in human Osteoarthritis chondrocytes. Free Radic Biol Med. 2017;106:288–301.
39. Lee SE, Park SH, Yoo JA, Kwon K, Kim JW, Oh SW, et al. Antagonizing Effects of Clematis apiifolia DC. Extract against Benzo[a]pyrene-Induced Damage to Human Keratinocytes. Oxid Med Cell Longev. 2019;2019:2386163.
40. Chen X, Yan L, Guo Z, Chen Z, Chen Y, Li M, et al. Adipose-derived mesenchymal stem cells promote the survival of fat grafts via crosstalk between the Nrf2 and TLR4 pathways. Cell Death Dis. 2016;7:e2369.

Figures

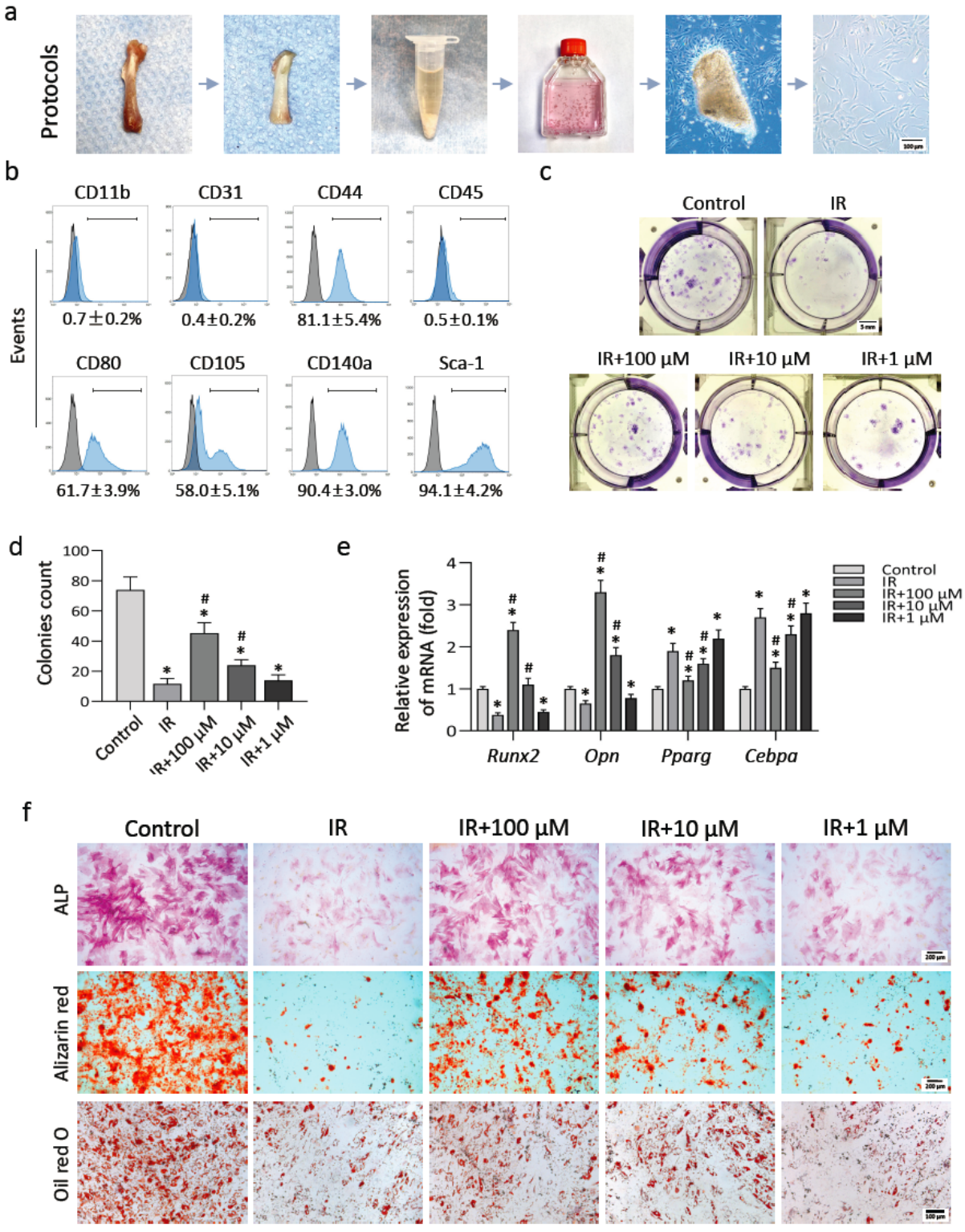

Figure 1

Effect of melatonin on self-renewal and multi-directional differentiation potential of postradiaiton CBSCs. a. Protocols for extracting CBSCs. b. Identification of CBSCs by flow cytometry. c.d. CFU-F assays and colonies count for detecting self-renewal ability. e. qRT-PCR analysis of osteogenic and adipogenic gene markers. f. ALP staining and Alizarin red staining after osteogenic induction. Oil red O staining after

adipogenic induction. *P < 0.05 compared with control; #P < 0.05 compared with IR. IR: irradiation; IR+100(10/1) μM: 100(10/1) μM melatonin treatment from 1 hour after irradiation for 24 hours.

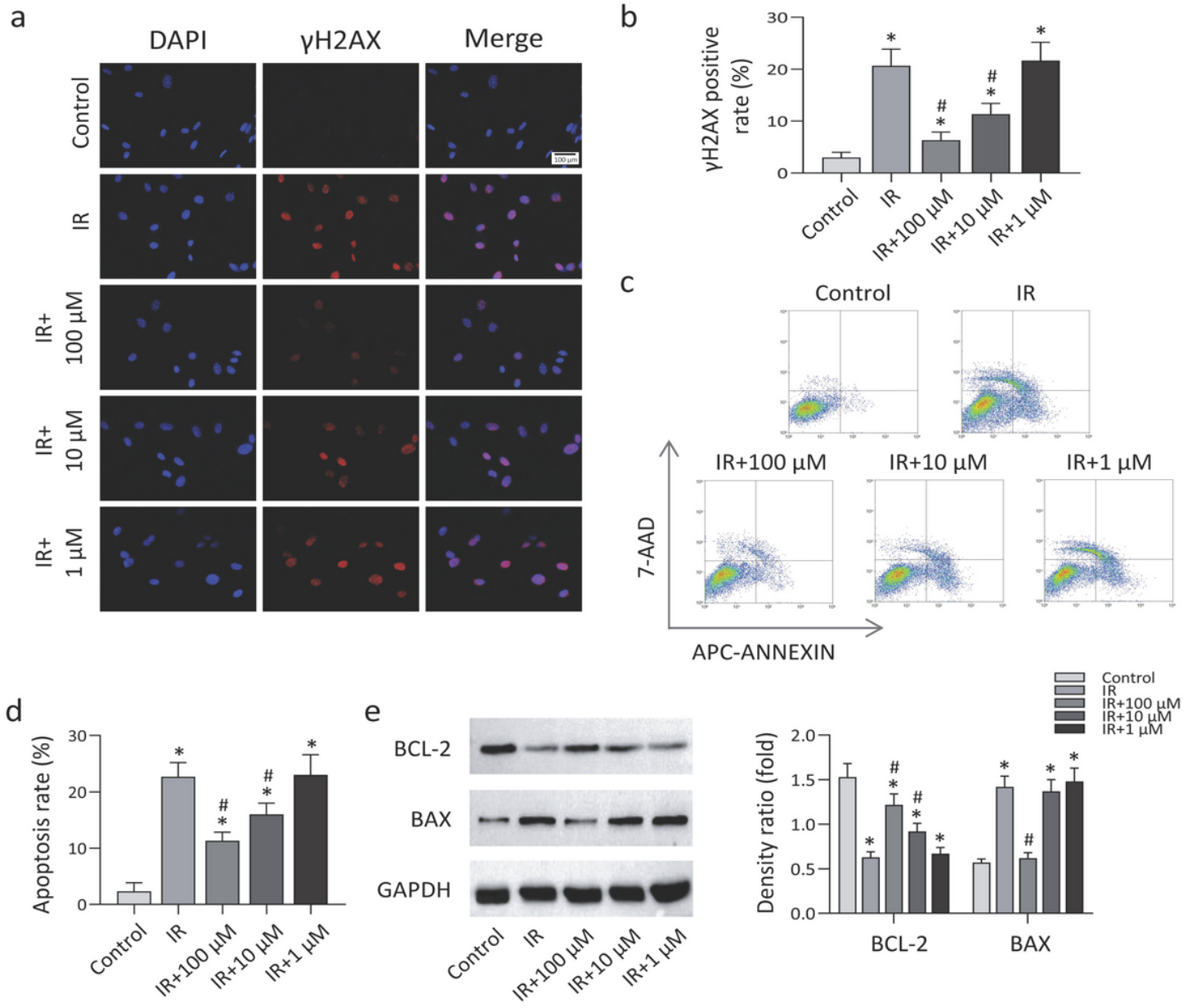

Figure 2

Effect of melatonin on DNA damage and apoptosis of postradiation CBSCs. a.b. Analysis of DNA breaks using γH2AX immunostaining. DAPI (blue) and γH2AX (red). c.d. Analysis of apoptosis by flow cytometry. e. The levels of anti-apoptotic protein BCL-2 and pro-apoptotic protein BAX were measured by western blotting. *P < 0.05 compared with control; #P < 0.05 compared with IR.

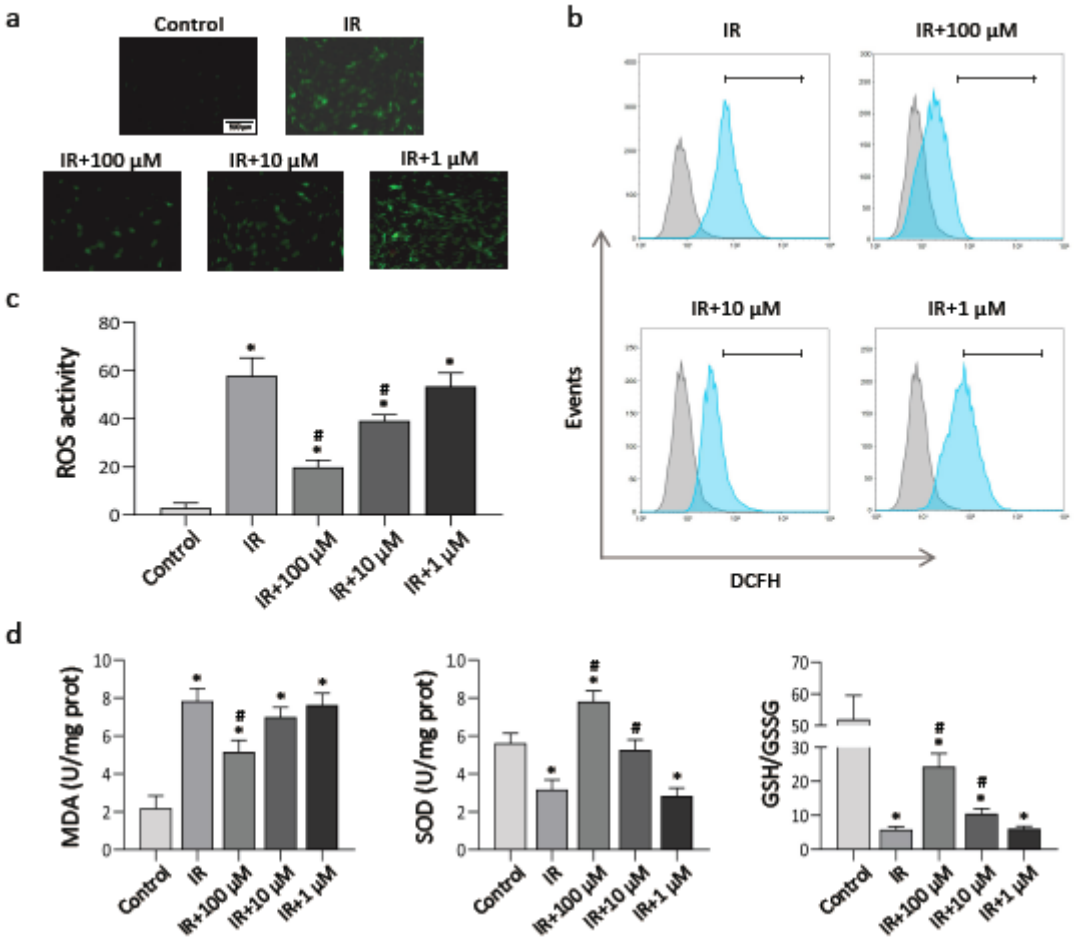

Figure 3

Effect of melatonin on intracellular oxidative stress in postradiation CBSCs. a.b.c. Intracellular ROS levels were detected and quantified by flow cytometry after DCFH-DA staining. d. The levels of oxidative stress-related markers in CBSCs. *P < 0.05 compared with control; #P < 0.05 compared with IR.

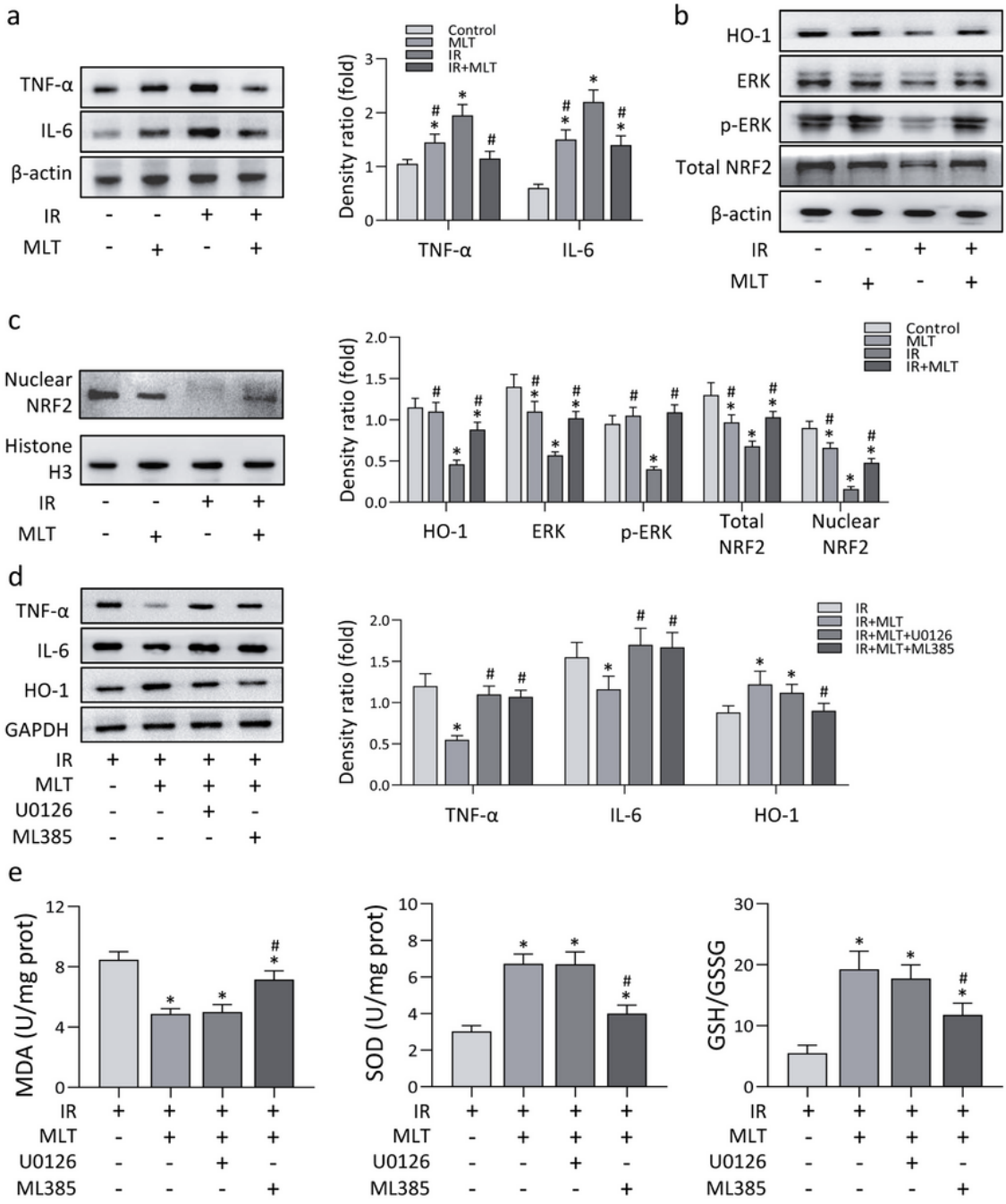

Figure 4

Melatonin activated ERK/NRF2/HO-1 signaling pathway in postradiation CBSCs. a. The levels of TNF-α and IL-6 in CBSCs were detected by western blotting. b.c. Intracellular markers of ERK/NRF2/HO-1 signaling were measured by western blotting. *P < 0.05 compared with control; #P < 0.05 compared with IR. d. The levels of HO-1, TNF-α and IL-6 were detected after postradiation CBSCs were treated with melatonin and inhibitors. e. The levels of oxidative stress-related markers were measured after

postradiation CBSCs were treated with melatonin and inhibitors. *P < 0.05 compared with IR; #P < 0.05 compared with IR+MLT.

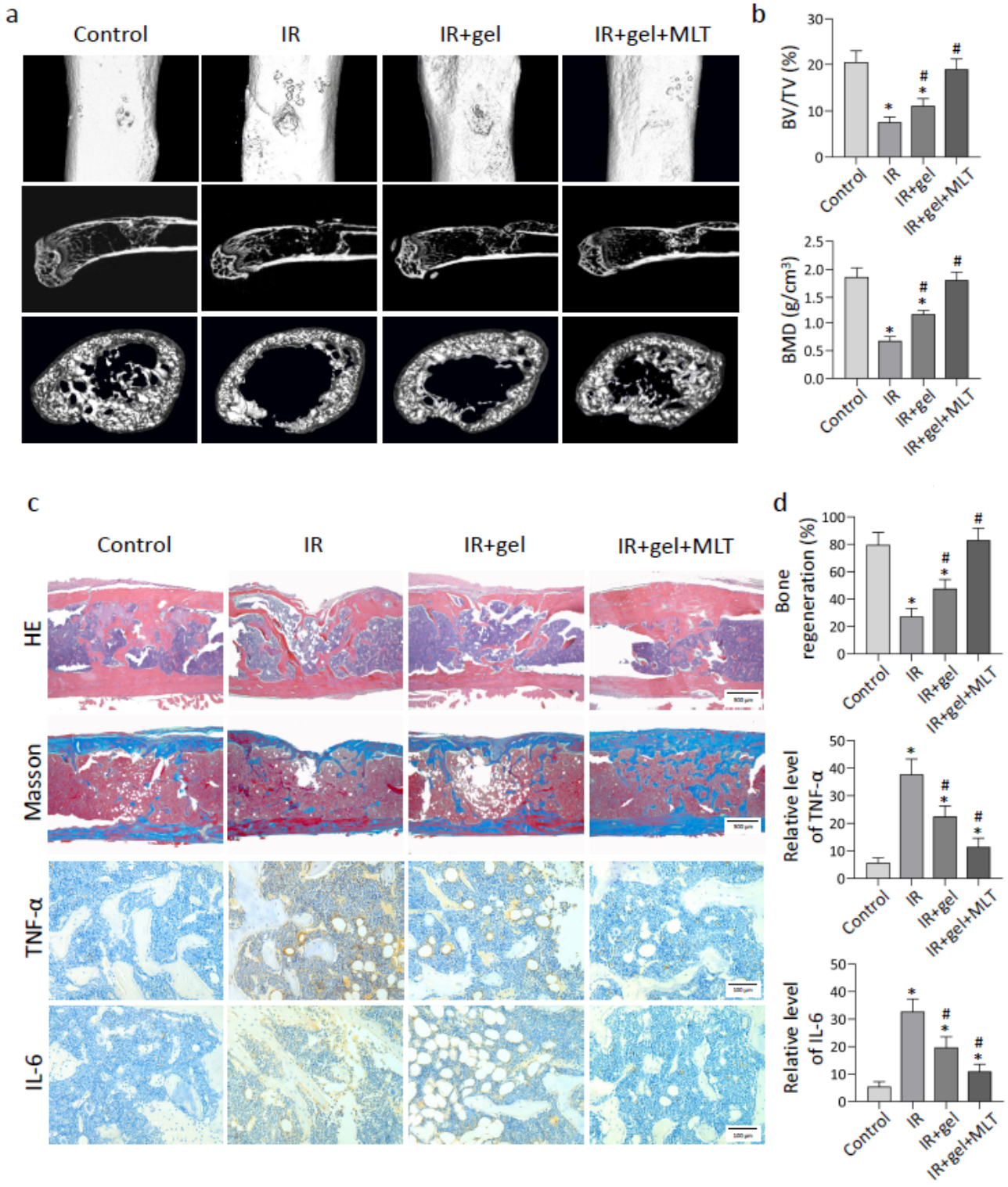

Figure 5

Melatonin benefited bone healing in a postradiation femoral defect model. a.b. Representative three-dimensional images and quantitative analysis of micro-CT. c.d. Representative images of HE staining,

Masson staining and immunochemical staining. Quantitative analysis was performed. *P < 0.05 compared with control; #P < 0.05 compared with IR.